RFHUI: An Intuitive and Easy-to-Operate Human-UAV Interaction System for Controlling a UAV in a 3D Space

Jian Zhang
RFID Lab, Auburn University
Auburn, AL
jzz0043@tigermail.auburn.edu

Zhitao Yu
Dept. ECE & RFID Lab, Auburn University
Auburn, AL
zzy0021@tigermail.auburn.edu

Xiangyu Wang
Dept. ECE & RFID Lab, Auburn University
Auburn, AL
xzw0042@tigermail.auburn.edu

Yibo Lyu
Dept. ECE & RFID Lab, Auburn University
Auburn, AL
yzl0113@tigermail.auburn.edu

Shiwen Mao
Dept. ECE, Auburn University
Auburn, AL
smao@ieee.org

Senthilkumar CG Periaswamy
RFID Lab, Auburn University
Auburn, AL
senthil@auburn.edu

Justin Patton
RFID Lab, Auburn University
Auburn, AL
jbp0033@auburn.edu

Xuyu Wang
Dept. ECE, Auburn University
Auburn, AL
XZW0029@tigermail.auburn.edu

ABSTRACT

With the increasing commercial prospect of personal Unmanned Aerial Vehicle (UAV), human and UAV interaction has been a compelling and challenging task. In this paper, we present the RFHUI, a human and UAV interaction system based on passive radio-frequency identification (RFID) technology which provides a remote control function. Three or more Ultra high frequency (UHF) RFID tags are attached on a board to create a hand-held controller. A COTS (Commercial Off-The-Shelf) RFID reader with multiple antennas is deployed to collect the observations of the tags. According to the phase measurement from the RFID reader, we leverage a Bayesian filter based method to localize the position of all tags in a global coordinate. From the estimated position of the attached tags, a 6 DOF (Degrees of Freedom) pose of the controller can be obtained. Therefore, when the user moves the controller, its pose will be precisely tracked in a real-time manner. Then, the flying commands, which are generated from the estimated pose of the controller, are sent to the UAV for navigation. We implemented a prototype of the RFHUI, and the experiment results show that it provides precise poses with 0.045 m error in position and 2.5° error in orientation for the controller. It therefore enables the controller to precisely and intuitively instruct the UAV's navigation in an indoor environment.

MobiQuitous '18, November 5–7, 2018, New York, NY, USA

ACM ISBN 978-1-4503-6093-7/18/11…$15.00
DOI: 10.1145/3286978.3286983

CCS CONCEPTS

• **Human-centered computing → Human computer interaction (HCI)**; • **Information systems →** *Information systems applications*;

KEYWORDS

RFID, HCI (Human Computer Interaction), UAV (Unmanned Aerial Vehicle), Localization

ACM Reference Format:
Jian Zhang, Zhitao Yu, Xiangyu Wang, Yibo Lyu, Shiwen Mao, Senthilkumar CG Periaswamy, Justin Patton, and Xuyu Wang. 2018. RFHUI: An Intuitive and Easy-to-Operate Human-UAV Interaction System for Controlling a UAV in a 3D Space. In *EAI International Conference on Mobile and Ubiquitous Systems: Computing, Networking and Services (MobiQuitous '18), November 5–7, 2018, New York, NY, USA.* ACM, New York, NY, USA, 8 pages. https:

1 INTRODUCTION

Use of the unmanned aerial vehicle (UAV), which originated in the military arena, has rapidly expanded to other areas, such as agriculture, research, commerce and more. Due to its prominent maneuverability, small size and low cost, the UAV is widely adopted for surveillance, entertainment, search and rescue, and inspection for maintenance. In terms of personal UAV application, over the past few years, many advanced algorithms and sensors have been introduced, making UAV use increasingly powerful and comprehensive. These personal UAVs are chiefly used for human entertainment activities, such as taking photos and videos. The mounting growth of demand makes the interaction between UAV and user become a research topic of considerable interest.

In this paper, we propose the RFID-based human UAV Interaction (RFHUI) - a low-cost, RFID-based system which will provide an intuitive and easy way to control and navigate a UAV in a complex indoor environment. The proposed method provides a means to precisely control a UAV to navigate in a 3D space in real-time. We attach N (N≥3) UHF passive RFID tags to a board to create a hand-held controller. We record the position of each tag against the built-in coordinate of the controller, this position is denoted as a local one. We deploy a COTS (Commercial Off-The-Shelf) RFID reader with multiple antennas to gather the observation of the tags. The global position, which refers to the global coordinate of the 3D space, of an RFID tag can be precisely tracked by the phase measurement of the RFID tag from multiple antennas. A 6DoF pose of the controller can be obtained from the known local position and estimated global position of the N attached tags. Finally, following the movement of the controller, the UAV responds and updates its pose. The main contributions of this work can be summarized as follows:

1. A real-time RFID tag localizer is created. Through the phase measurement from a COTS reader, it localizes multiple UHF RFID tags simultaneously.

2. A real-time pose tracker is proposed. Based on the position of the attached tags, a precise 6DoF pose for the controller is estimated in a 3D space.

3. We convert the pose of the controller into the flying commands of the UAV for navigation.

4. We implement the RFHUI system with the COTS RFID device and demonstrate its performance in a representative indoor environment. Experimental results show that the RFHUI can provide precise poses with 0.045 m error in position and 2.5° error in orientation for the controller, thus, it enables the controller to precisely and intuitively instruct the UAV's navigation in an indoor environment.

The remainder of this paper is organized as follows. We review related work in Section 2. We present the approach and analysis of the RFHUI system in Section 3 and our experimental study in Section 4. Section 5 concludes this paper.

2 RELATED WORK

With the development of robotics and growing demands for civilian and industry applications, the concept of interaction and collaboration between human and robots has received a lot of attention. The study of Human-Robot Interaction(HRI) focuses on how their communication creates better real-time performance of tasks. It can be approximately divided into three areas of application: teleoperation in the specific environment [1][2], human-centric social interaction[3] and industry-needed manufactories[4]. For applications in social interaction, Santos et al. proposed a tour-guide robot which is capable of recognizing users hand gestures and providing voice feedback [5]. In the field of HRI teleoperation in a specific environment, urban search and rescue(USAR) is a high interest research topic for deploying an HRI teleoperation in a specific environment. For example, Kohlbrecher et al. presented a human-robot system for rescue missions [6].

Compared to the traditional robotic Unmanned Ground Vehicle (UGV), the UAV has significant differences, including flying freely, poor carrying capability and being unsafe to touch. This demands a different and suitable new interaction method for humans and UAVs. The applications of Human-Drone Interaction (HDI) primarily focused on jogging companion UAVs invovled in filming videos, gesture recognition and floating display. Muller et al. designed and built an outside jogging companion quadcopter system[7] based on GPS localization. Additionally, Scheible et al. proposed a system that combines a quadrocopter, a video projector and a mobile phone for projecting contents onto walls or objects in an open space [8]. Obviously, these UAVs are large and could only be used outside, prohibiting close interaction between human and drones. For the gesture control applications, Cauchard et al. made an investigation of multiple participants and illustrated that natural gesture control leads to a more intimate relationship between UAVs and users[9]. In the current commecial UAV market, DJI unveiled a state-of-the-art small gesture control-based UAV product, Spark[16], in May 2017. This is the first time gesture recognition technologies have been introduced in consumer-class UAVs, enabling the removal of a traditional remote controller.

Since the last decade, RFID technology has been widely recognized as a promising solution for item serialization and tracking. Due to its cost-effective, lightweight and powerless properties, the RFID has also been widely deployed for indoor localization[17] [23]. A considerable number of studies have focused on accessing phase measurement of RF signals for localization[18] [19]. Making use of Angle of Arrival(AOA) is a classic solution which is driven by measuring the phase difference of the signals received at different antennas. In [20], Azzouzi presented the new measurement results for an AOA approach to localize RFID tags. In addition to localization applications, RFID technology has also been employed for 3-D reconstruction. Bu et al. proposed an approach based on the phase differences of RF signals for 3-D reconstruction of cubes [21], which is free of the limitation of line-of-sight and the constraint on battery life . Moreover, there are many other interesting scenarios that access RFID technology. For example, the reading patterns of RFID tags are leveraged to detect customers' behaviors in a physical clothes store [22].

Motivated by the research of the aforementioned RFID applications, we go beyond HRI and HDI works to design a practical HDI navigation system based on RFID technologies and test it in a real-world laboratory environment. Compared to traditional vision-based HDI systems, the proposed RFHUI does not have the limitation of line-of-sight due to the penetrating characteristics of RF signals.

3 APPROACH AND ANALYSIS

RFHUI is a low-cost, RFID-enabled system aiming to offer novel human-UAV interaction. It provides an intuitive and easy-to-operate means for controlling a UAV in a 3D space. The RFHUI system comprises N ($N \geq 3$) UHF passive RFID tags and a COST RFID reader with M ($M \geq 2$) antennas. The tags are attached to the controller, and, when tracking the RFID tags by querying the phase information of each tag, a 6DoF pose of the controller can be obtained. Then, the UAV can be controlled by this pose. In this section, we will introduce the system model and RFHUI architecture.

3.1 System Architecture

The system architecture of the RFHUI is illustrated in the Fig 1.

There are three main components of our proposed system:

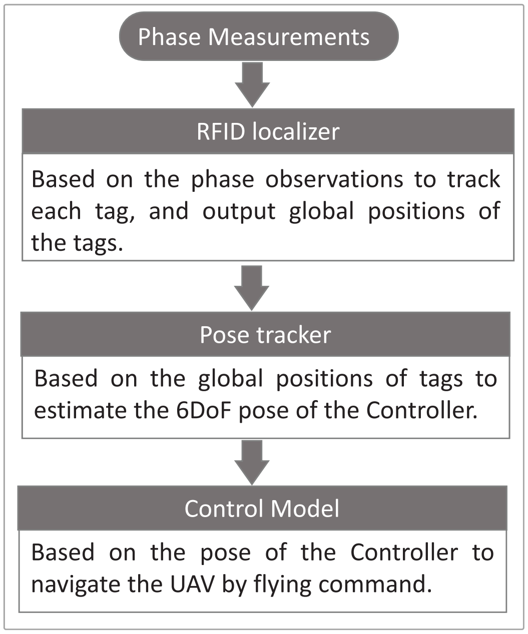

Figure 1: The system architecture of the RFHUI, here the global coordinate is built in the real world.

- **RFID localizer**: We deploy a Bayesian filter to estimate the global location of the tags by utilizing the phase measurement of each tag, which is obtained from the reader.
- **Pose tracker**: After the global location of N($N \geq 3$) tags are provided by the RFID localizer and combined with the given local location of each tag, we can track the pose of the controller with an SVD-based method. Here, the local location is given in the built-in coordinate of the controller.
- **Control Module**: It converts the pose of the controller into the flying commands and sends it to the UAV, thus, the UAV navigates in a trajectory that is guided by the movement of the controller.

3.2 RFID Localizer

In the RFHUI system, the phase measurement of the tags is collected by an RFID reader with M antennas. We fix and measure the positions of all antennas; hereafter, l_m denotes the position of the m_{th} antenna in the global coordinate.

Bayesian Filter Updating for Tag Localizing: A Bayesian filter is deployed to localize the tags. It addresses the problem of estimating belief over the hypothetical posterior state x of a dynamic system by sensor observations. For the RFID localizer, the state x denotes the position of the tag against the global coordinate. The belief bel(x_t), which denotes the probability that the system is on state x at time t, is recursively updated by the Bayesian filter. It is calculated from control u_t, observation z_t and prior belief $bel\,(x_{t-1})$ at time $t-1$, which is calculated previously. Usually, one updating cycle of a typical Bayesian filter can be divided into two essential steps. Control update or prediction is the first step of the process, which is illustrated by the equation:

$$\overline{bel}\,(x_t) = \int P\,(x_t|u_t, x_{t-1})\,bel\,(x_{t-1})\,dx_{t-1}, \tag{1}$$

where $P\,(x_t|\,u_t, x_{t-1})$ provides the probability of a tag move from the position x_{t-1} to x_t under the control of u_t, referred to as a motion model, and $\overline{bel}\,(x_t)$ represents the probability of the tag at position x_t after the control u_t is updated. We assume that the speed of tags will keep constant for a very short time interval, hence, a constant speed model can be deployed for the RFID localizer, which is expressed as:

$$P\,(x_t|u_t, x_{t-1}) = \frac{1}{\sqrt{2\pi}\delta}\int_0^{\Delta t} e^{-\frac{(x_t-(x_{t-1}+\,u_t\cdot y\,))^2}{2\delta^2}}\,dy, \tag{2}$$

where u_t denotes the speed of item at time $t-1$ and Δt represents the time interval between $t-1$ and t. The movements of the item satisfy a typical Gaussian distribution and δ is the standard deviation of it. The second step is the measurement update, which is illustrated by the equation:

$$bel\,(x_t) = \eta \cdot \overline{bel}\,(x_t)\,P\,(z_t|\,x_t). \tag{3}$$

In (3), η is a constant to integrate the sum of all $bel\,(x_t)$ into 1, and $P\,(z_t\,|\,x_t)$ represents the observation model. In our RFID localizer, we deploy M reader antennas, thus, the (3) can be rewritten as:

$$bel\,(x_t) = \sum_{m=1}^{M} \eta \cdot \overline{bel}\,(x_t)\,P\,(z_t|\,x_t, l_m), \tag{4}$$

where $P\,(z_t\,|\,x_t, l_m)$ denotes the observation model for the m_{th} antenna. It provides the probability of when the m_{th} antenna in position l_m observes the measurement z_t of the tag, which is in position x_t. The detail of the model is presented as follows.

Model of RFID Phase measurement: The relationship for the RF phase shift between sent and received signal is given by the following equation:

$$\theta = \left(2\pi \cdot \left(\frac{2R}{\lambda}\right) + \theta_T + \theta_R + \theta_{TAG}\right) \mod 2\pi, \tag{5}$$

where θ is the RF phase measured by the reader, R is the distance between the reader antenna and the RFID tag, $\theta_T, \theta_R, \theta_{TAG}$ are the RF phase distortion caused by the reader's transmit circuits, the reader's receiver circuits and tag's reflection characteristic, respectively, and *mod* is the Modulo operation. Experiments show that for the same reader antenna, the same RFID tag and the same radio frequency, $\theta_T, \theta_R, \theta_{TAG}$ are fixed, and can be denoted as $\theta' = \theta_T + \theta_R + \theta_{TAG}$. Thus, the equation (5) can be rewritten as:

$$\theta = \left(2\pi \cdot \left(\frac{2R}{\lambda}\right) + \theta'\right) \mod 2\pi. \tag{6}$$

We assume a tag in position x_{t-1} and a reader antenna in a position l_m observe the RF phase θ_1 for the tag. Under the same RF frequency, the tag moves to the position x_t and the RF phase θ_2 is obtained for the tag. The differential RF phase measurement between the two positions satisfies the following equation:

$$\Delta\theta_{12} = (\theta_1 - \theta_2)\ mod\ 2\pi. \tag{7}$$

$$\Delta\theta_{12} = \left(\left(2\pi\left(\frac{2\left|x_{t-1}l_m^g\right|}{\lambda}\right)+\theta'\right) mod\ 2\pi - \left(2\pi\left(\frac{2\left|x_t l_m^g\right|}{\lambda}\right)+\theta'\right) mod\ 2\pi\right) \mod 2\pi. \tag{8}$$

$$\Delta\theta_{12} = \left(\frac{4\pi}{\lambda}\cdot\left(|x_{t-1}l_m| - |x_t l_m|\right)\right) \mod 2\pi. \tag{9}$$

Equation (9) shows that under the same frequency for the same antenna and the same RFID tag, the differential RF phase $\Delta\theta_{12}$ is only determined by the distance the tag moves from x_{t-1} to x_t. $|x_t l_m|$ denotes the distance between the two positions. Hereafter, we assume that the all the RF phases are measured for the same RFID reader and the same RFID tag under the same RF frequency. The tag moves in a discrete trajectory that is represented by a series of locations $x1, x2,$ fi$, xt$. The antenna, which is stationary in position l_m, collects the phase measurement in each location as $\theta_1, \theta_2,$ fi$, \theta_m$. Then, the discrete trajectory of the movement of the tag should satisfy:

$$\begin{cases} |x_i l_m| - |x_j l_m| = \frac{\lambda}{4\pi}\,\Delta\theta_{ij} + n\,\frac{\lambda}{2} \\ \Delta\theta_{ij} = (\theta_i - \theta_j)\ mod\ 2\pi \\ n \in \{1,\ 2,\ 3,\ \ldots\} \\ i, j \in \{1, 2, \ldots, t\} \text{ and } i \neq j. \end{cases} \tag{10}$$

The observation model $P(z_t \mid x_t, l_m)$ can be updated by the (10) to provide the probability that if a tag moves from x_{t-1} to x_t, the differential RF phase $\Delta\theta_{t,t-1}$ is obtained by the reader. We model the differential RF phase by the following equation:

$$P\left(\Delta\theta_{t,t-1}\middle| x_{t-1}, x_t, l_m\right) = \begin{cases} 1, & \text{if (10) is satisfied} \\ 0, & \text{otherwise.} \end{cases} \tag{11}$$

Let's consider the distortion of the RF phase that is caused by the thermal noise. Experiments reveal that the thermal noises bring random errors to the phase measurement with a typical Gaussian distribution. Thus, we can denote the RF phase as $\theta \sim \mathcal{N}(\mu, \delta)$, where μ is the RF phase without the distortion of thermal noise and δ denotes the standard deviation. Hence, we can update the differential RF phase as $\Delta\theta_{ij} \sim \mathcal{N}(\mu_i - \mu_j, \sqrt{2}\delta)$, and the equation (11) can be updated as:

$$\begin{cases} P\left(\Delta\theta_{t,t-1}|x_{t-1}, x_t, l_m\right) = \frac{1}{\sqrt{2\pi}\delta}\int_0^{\Delta\theta_{t,t-1}} e^{-\frac{(y-(\mu_t-\mu_{t-1}))^2}{2\delta^2}}dy \\ \mu_t - \mu_{t-1} = \left(\frac{2|x_t l_m|}{\lambda} - \frac{2|x_{t-1} l_m|}{\lambda}\right) \mod 2\pi, \end{cases} \tag{12}$$

where λ is the wave length of the RF radio signal. Based on equations (12) and (4), we can estimate the location of RFID tags.

3.3 Pose Tracker

The location of the tags, which is denoted $p_n^t = (x_n^t, y_n^t, z_n^t)^T$ of the n_{th} tag at the time t, can be provided by the RFID localizer. When the controller is located at T, with orientation R in the given global coordinate, the T and the R together are called the pose of the controller. Here, we denote the position of the camera as

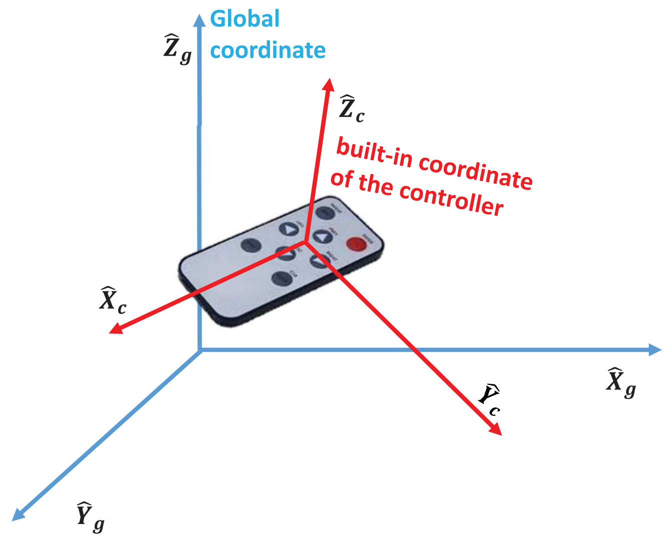

Figure 2: Global Coordinate vs Built-in Coordinate of the controller.

$T_t = (x_t, y_t, z_t)^T$, and the orientation as

$$R_t = \begin{bmatrix} \hat{X}_c \cdot \hat{X}_g & \hat{Y}_c \cdot \hat{X}_g & \hat{Z}_c \cdot \hat{X}_g \\ \hat{X}_c \cdot \hat{Y}_g & \hat{Y}_c \cdot \hat{Y}_g & \hat{Z}_c \cdot \hat{Y}_g \\ \hat{X}_c \cdot \hat{Z}_g & \hat{Y}_c \cdot \hat{Z}_g & \hat{Z}_c \cdot \hat{Z}_g \end{bmatrix}, \tag{13}$$

where $\hat{X}_c, \hat{Y}_c$ and $\hat{Z}_c$ represent the unit vectors of the axis of the built-in coordinate of the controller, and $\hat{X}_g$, $\hat{Y}_g$ and $\hat{Z}_g$ denote the unit vectors of the axis in the global coordinate. The relationship of the two coordinates is illustrated in Fig 2. We measure the location of each attached tag in the controller's built-in coordinate, and the local location for the n_{th} tag is denoted as $\bar{p_n} = (\bar{x_n}, \bar{y_n}, \bar{z_n})^T$. The transformation between the global location and local location of the same tag is

$$\begin{cases} P_n^t = {}^g_cT_t \cdot \bar{P_n} \\ P_n^t = (p_n^t, 1)^T \\ \bar{P_n} = (\bar{p_n}, 1)^T \end{cases} \tag{14}$$

where ${}^g_cT_t$ denotes the rigid transform at time t, p_n^t and $\bar{p_n}$ is the location of the n_{th} tag in the global coordinate and the controller built-in coordinate, respectively. The ${}^g_cT_t$ comprises the pose of the controller's in the global coordinate:

$${}^g_cT_t = \begin{bmatrix} R_t & T_t \\ 0\,0\,0 & 1 \end{bmatrix}, \tag{15}$$

where $R_t$and T_t denote the global orientation and global position of the controller at time t, respectively.

3.4 Human UAV Interaction Module

The human UAV interaction module primarily links the change of the controller's pose with UAV movement to achieve the remote control. Based on the estimated pose of the controller, it controls the navigation of the UAV. To achieve real-time control, the UAV

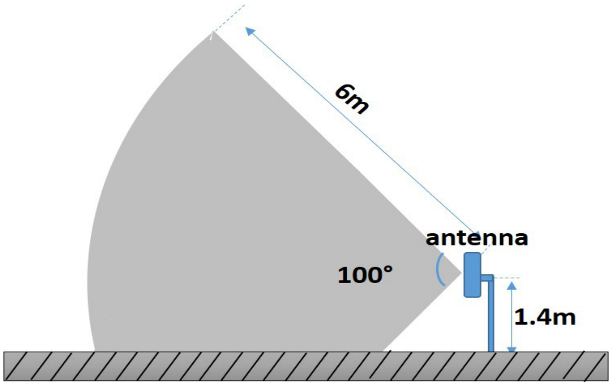

Figure 3: The Side view of the RFID detectable field.

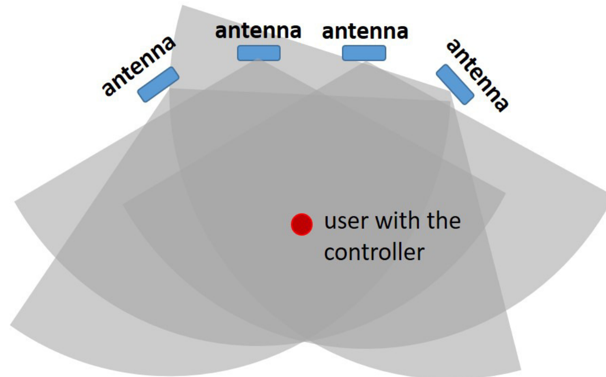

Figure 4: The top view of the RFID detectable field.

must react sensitively to the change of the controller's pose in a manner which follows the trajectory of the moving controller. We use $H_t = (x_t, y_t, z_t, r_t, p_t, y_t)$ to denote the pose of the controller and the pose of UAV at time t is denoted as U_t. The process of the module can be divided into four steps, which are detailed as follows:

1. Getting H_t and H_{t+1} from the pose tracker.
2. Calculating the $\Delta H = H_{t+1} - H_t$ which contains the change of position and orientation in the three-dimensional space.
3. Amplifying the ΔH as $\Delta H^{'} = N \times \Delta H$, here, N is the parameter of the amplification, and we usually set N=5. We can use a slight movement of the controller to activate a large-scale movement of the UAV.
4. Converting the $\Delta H^{'}$ to the flying commands and send to the UAV.

The step 4 coorperates with the specific UAV platform, and it usually relies on the API to communicate with the UAV. For example, in our experimental platform, it is implemented on the ROS system [24] to communicate with the ARDrone2.0 platform [10]. It updates the target position of the UAV by $U_{t+1} = U_t + \Delta H^{'}$, and send the U_{t+1} to the UAV through the ROS message services.

4 EXPERIMENTAL RESULTS

4.1 Experiment Setup

We conducted a series of experiments to demonstrate the performance of the RFHUI system. We established a prototype of the RFHUI using a COTS reader and several UHF passive RFID tags. A Zebra FX7500 RFID reader[11] with four Zebra AN720 antennas[12] is implemented to query the RFID tags. The Zebra FX7500 reader is widely deployed in retail, manufacture factory and warehouse,and meets the EPC Gen2[13] standard. In our prototype system, we use the Low-Level Reader Protocol (LLRP) through an Ethernet port to communicate with the reader and report the RFID measurements. The Zebra AN720 Antennas provide a left circular polarization with 100° beam width and a 5.5 ∼ 6 dB gain. Each antenna is mounted on a holder of 1.4 m height. The four antennas with their holders are deployed in front of the user. For all our experiments, we set the reader works at the maximum RF transmission power, 33 dBm, to enable each antenna to gain a detectable range up to 6m. Our experiment setting is shown in Fig 3 and Fig 4.

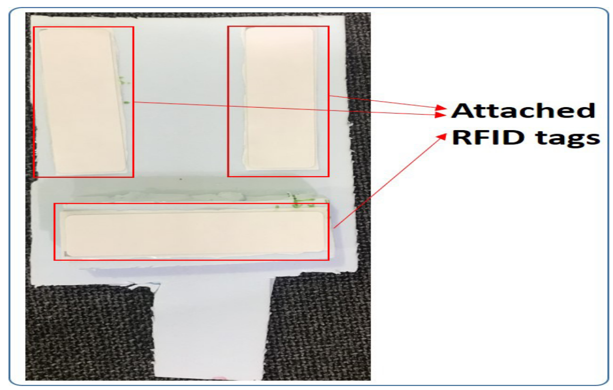

Figure 5: A prototype of our RFHUI controller.

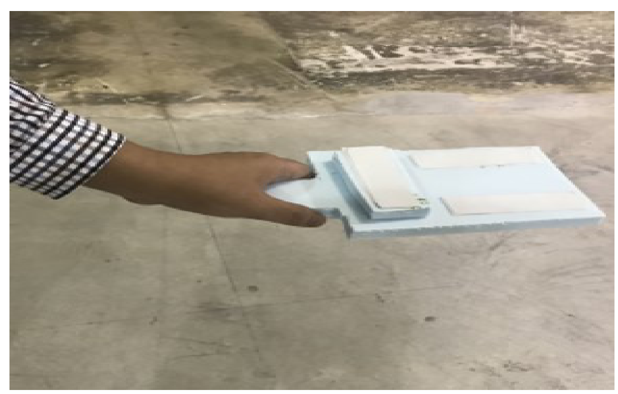

Figure 6: A user holds the controller.

The configuration of the four antennas created a detectable field to enable an RFID tag which could be interrogated by the four antennas simultaneously.

Three UHF passive RFID tags are attached to a foam board works as our prototype controller and is shown in Fig 5. The Fig 6 shows how the controller is operated by a user during the tests. Our experimental RFID tag is Smartrac Dogbone Monza R6[14], which is widely used in the retail. We choose The Parrot ARDrone2.0 Elite

Figure 7: The ARDrone2.0 Elite Edition.

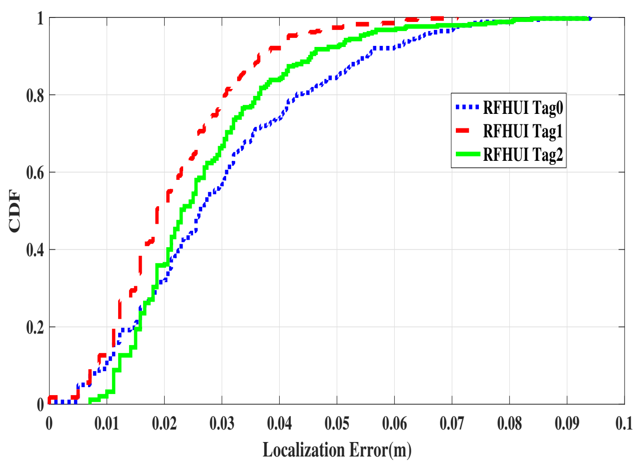

Figure 8: CDF of RFID Tags Tracking Error.

Edition[15] as our UAV platform, which is shown in Fig 7. It equips a front camera, a bottom camera, a sonar and an IMU, and based on the measurements of the onboard sensors, it can localize itself by using a sensor fusion method. For example, the Parallel Tracking and Mapping (PTAM) [16] can be implemented to estimate the 3D pose of the ARDrone2.0.

4.2 The accuracy of RFID tracking and Pose Estimation

4.2.1 RFID tags tracking: First, to evaluate the performance of the RFID localizer of the RFHUI, we launched an experiment by attaching three UHF passive RFID tags to the controller. A user held the controller and moved it using a given trajectory, which was inside of the experiment field. During the experiment, the RFID localizer of the RFHUI provided estimated locations for each tag while the controller was moving. We obtained the ground-truth locations by measuring the sampled points along the trajectory. The accuracy of the proposed method is evaluated by calculating the errors between the ground-truth locations and the estimated locations of the sampled points. The experimental result is shown by the Fig 8. It presents the cumulative distribution function (CDF)

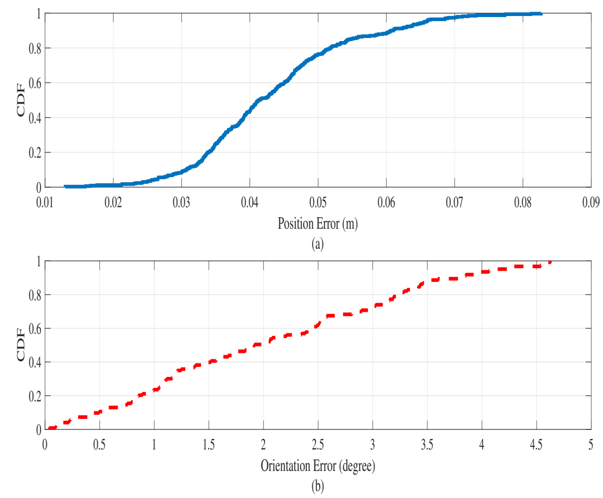

Figure 9: (a) CDF of Controller Position Estimation Error, (b) CDF of Controller Orientation Error

of localization errors between estimated and ground-truth positions. We can tell that the maximum error of the RFID localizer is less than 0.095m for all three tags. Moreover, the RFID localizer of the RFHUI provides 80% of localization errors less than 0.045m and 90% of them are under 0.06m. Therefore, it is safe to state that the RFID localizer provides a very precise localization for the tracking of the moving RFID tags.

4.2.2 Controller Pose Estimation: Second, we implemented an experiment to verify the feasibility and accuracy of our proposed pose tracker, including position and orientation estimation. The controller moved along a trajectory in our experiment field, while a user held it. The results are given in Fig 9. Fig 9(a) shows that about 78% of position errors for the proposed pose tracker are under 0.05m, and the maximum error is less than 0.083m. Additionally, as shown by Fig 9(b), we can tell that there are 60% orientation errors less than 2.5 in degree. Moreover, the pose tracker has almost 90% orientation estimations achieving an error under 3.5 in degree. Obviously, regardless of position and orientation estimation, the proposed pose tracker of the RFHUI is practicable for human-UAV interaction.

4.3 System Performance

Finally, we conducted an experiment in our Lab indoor environment to demonstrate the feasibility of our system in a real-time manner. The typical experimental environments are shown in Fig 10 and Fig 11. The complex indoor environment, such as the intricate features and layouts of the shelves, clothes stands and furniture in Fig 11, requires our proposed RFHUI system to provide an accurate and robust control method to safely operate the UAV. During the experiment, a user held the controller, which is attached with 3 RFID tags, to control the UAV. We compared the ideal movement trajectory of the UAV, which is amplified by the trajectory of the controller, and the actual movement of the UAV to illustrate the performance of the proposed RFHUI. A typical experiment result is illustrated by Fig 12. The movement of the controller followed

Figure 10: Empty Lab Environment.

Figure 11: Complicated Lab Environment.

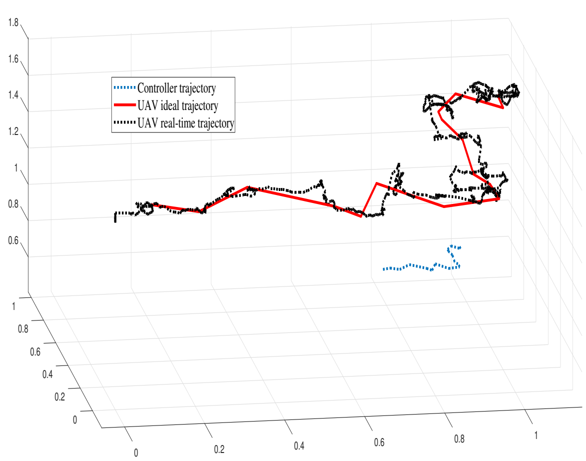

Figure 12: Trajectory Comparison

a random trajectory, which is illustrated by the blue curve in the Fig 12. The red curve denotes the amplified ideal trajectory of the UAV according to the movement of the controller. Clearly, we can tell that the UAV precisely follows the ideal trajectory, only a tiny disturbance around the ideal occurred. This is caused by inherent errors of the UAV, especially, when the UAV is in a hovering mode. It is apparent that our RFHUI system achieves high accuracy in real-time following, which proves our RFID-based controller strategy is robust and practicable. This is mainly due to the the fact that our proposed RFHUI system can provide a highly accurate pose estimation, which plays a critical role in controlling the UAV navigation.

5 CONCLUSIONS

In this paper, we propose the RFHUI, an RFID based system for the navigating control of the UAV using a COTS RFID reader. We experimentally validate the feasibility of utilizing an RFID localization-based method as the core of the UAV controller. We leverage a Bayesian filter to access the estimated location of RFID tags with its phase information. Then, for the last step of data pre-processing, an SVD algorithm is provided for tracking the pose of the controller. Finally, the control module converts the pose data into flying commands to achieve the UAV navigation control purpose. The comprehensive experiments demonstrated the capability of the proposed RFHUI system. To the best of our knowledge, proposed RFHUI is the first practicable UHF passive RFID based UAV navigation control system which provides a promising method for Human-UAV interaction.

ACKNOWLEDGMENTS

This work is supported in part by the US NSF under Grant CNS-1702957, and by the Wireless Engineering Research and Education Center (WEREC) at Auburn University.

REFERENCES

[1] J. L. Casper and R. R. Murphy, "Workflow study on human-robot interaction in USAR," Robotics and Automation, no. May, pp. 1997-2003, IEEE, 2002.
[2] H. Jones, S. Rock, D. Burns, and S. Morris, Autonomous robots in swat applications: Research, design, and operations challenges," Auvsi'02, 2002.
[3] C. Bartneck and J. Forlizzi, "A design-centered framework for social human-robot interaction," International Workshop on Robot and Human Interactive Communication , pp. 591-594, 2004.
[4] W. Fkdoohqjhv et al.,"safe and reliable human-robot interaction in manufactory, within and beyond the workcell," pp. 65-70, 2010.
[5] V. Alvarez-Santos, R. Iglesias, X. M. Pardo, C. V. Regueiro, and A. Canedo-Rodriguez, "Gesture-based interaction with voice feedback for a tour-guide robot," Journal of Visual Communication and Image Representation, vol. 25, no. 2, pp. 499-509, 2014.
[6] J. Montgomery, S. I. Roumeliotis, A. Johnson, and L. Matthies, "Human-robot Teaming for Rescue Missions: Team ViGIR's Approach to the 2013 DARPA Robotics Challenge Trials," J.Field Robotics, vol. 23, no. 3, pp. 245-267, 2006.
[7] F."Floyd" Mueller and M. Muirhead, "Jogging with a Quadcopter," Proceedings of the ACM CHI'15 Conference on Human Factors in Computing Systems, vol. 1, pp. 2023-2032, 2015.
[8] J. Scheible, A. Hoth, J. Saal, and H. Su, "Displaydrone: A Flying Robot Based Interactive Display,"ï£¡ Proceedings of the 2nd ACM International Symposium on Pervasive Displays - PerDis'13, p. 49, 2013.
[9] J. R. Cauchard, J. L. E. Kevin, Y. Zhai, and J. A. Landay, "Drone & Me: An Exploration Into Natural Human-Drone Interaction," UbiComp '15, pp. 361-365, 2015.
[10] Parrot ARDrone2.0, [online] Available: https://www.parrot.com/global/drones/parrot-ardrone-20-elite-edition#parrot-ardrone-20-elite-edition. Accessed on June. 4, 2018.
[11] Zebra, fx7500, [online] Available: https://www.zebra.com/us/en/products/rfid/rfid-readers/fx7500.html. Access on June. 4, 2018.
[12] Zebra, an720, [online] Available: https://www.zebra.com/us/en/products/rfid/rfid-reader-antennas/an720.html. Accessed on June. 4, 2018.
[13] GS1 US, [online] Available: https://www.gs1us.org/. Accessed on June. 4, 2018.

[14] Samrtarc, Dogbone, [online] Available: https://www.smartrac\protect\discretionary{\char\hyphenchar\font}{}{}group.com/files/content/Products_Services/PDF/0028_SMARTRAC_DOGBONE.pdf. Accessed on June. 4, 2018.
[15] D. M. Klein, Georg,"Parallel Tracking and Mapping for Small AR Workspaces," Mixed and Augmented Reality, 2007. ISMAR 2007. 6th IEEE and ACM International Symposium on, pp. 225-234, 2007.
[16] DJI,SPARK, [online] Available: https://www.dji.com/spark. Accessed on June. 4, 2018.
[17] J. Zhang, Y. Lyu, J. Patton, S. Chinnappa Gounder P, and T. Roppel, BFVP: A Probabilistic UHF RFID Tag Localization Algorithm Using Bayesian Filter and a Variable Power RFID Model, *IEEE Transactions on Industrial Electronics*, 2018.
[18] Z. Yanjun,ï£¡ï£¡ Survivable RFID Systems: Issues, Challenges, and Techniques,*IEEE Transactions on Systems, Man, and Cybernetics, Part C (Applications and Reviews)*, vol. 40, no. 4, pp. 406âĂŞ418, 2010.
[19] S. Azzouzi, M. Cremer, U. Dettmar, R. Kronberger, and T. Knie, âĂIJNew measurement results for the localization of UHF RFID transponders using an Angle of Arrival (AoA) approach, *RFID (RFID), 2011 IEEE International Conference on*, pp. 91âĂŞ97, 2011.
[20] Azzouzi, Salah, et al. "New measurement results for the localization of uhf rfid transponders using an angle of arrival (aoa) approach," RFID (RFID), 2011 IEEE International Conference on. IEEE, 2011.
[21] Y. Bu, L. Xie, J. Liu, B. He, Y. Gong, and S. Lu, 3-Dimensional Reconstruction on Tagged Packages via RFID Systems, 2017 14th Annual IEEE International Conference on Sensing, Communication, and Networking, SECON 2017, 2017.
[22] Zhou, Zimu, et al. "Design and implementation of an RFID-based customer shopping behavior mining system." IEEE/ACM Transactions on Networking 25.4 (2017): 2405-2418.
[23] T. M. Choi, ?Coordination and risk analysis of VMI supply chains with RFID technology,? *IEEE Trans. Ind. Informat.*, vol. 7, no. 3, pp. 497?504, Aug. 2011.
[24] ROS,[online] Available: http://www.ros.org/. Accessed on June. 4, 2018.